






Quality and Precision for Stem Cell Purification

Deriving precursor cells from embryonic and induced pluripotent stem cells is no trivial task. Discover how researchers across the world have used the Sony MA900 Multi-Application Cell Sorter to empower their stem cell research.

[**Download Publications List**](#)

SONY

Research Article**Bruton's tyrosine kinase inhibition induces rewiring of proximal and distal B-cell receptor signaling in mice**

*Jasper Rip*¹ , *Marjolein J. W. de Bruijn*¹, *Stefan F. H. Neys*¹,
*Simar Pal Singh*¹, *Jonas Willar*², *Jennifer A. C. van Hulst*¹,
Rudi W. Hendriks^{#1}  and *Odilia B. J. Corneth*^{#1} 

¹ Department of Pulmonary Medicine, Erasmus MC, University Medical Center, Rotterdam, The Netherlands

² Department of Biology, Institute of Genetics, University of Erlangen-Nuremberg, Erlangen, Germany

Bruton's tyrosine kinase (Btk) is a crucial signaling molecule in BCR signaling and a key regulator of B-cell differentiation and function. Btk inhibition has shown impressive clinical efficacy in various B-cell malignancies. However, it remains unknown whether inhibition additionally induces changes in BCR signaling due to feedback mechanisms, a phenomenon referred to as BCR rewiring. In this report, we studied the impact of Btk activity on major components of the BCR signaling pathway in mice. As expected, NF- κ B and Akt/S6 signaling was decreased in Btk-deficient B cells. Unexpectedly, phosphorylation of several proximal signaling molecules, including CD79a, Syk, and PI3K, as well as the key Btk-effector PLC γ 2 and the more downstream kinase Erk, were significantly increased. This pattern of BCR rewiring was essentially opposite in B cells from transgenic mice overexpressing Btk. Importantly, prolonged Btk inhibitor treatment of WT mice or mice engrafted with leukemic B cells also resulted in increased phospho-CD79a and phospho-PLC γ 2 in B cells. Our findings show that Btk enzymatic function determines phosphorylation of proximal and distal BCR signaling molecules in B cells. We conclude that Btk inhibitor treatment results in rewiring of BCR signaling, which may affect both malignant and healthy B cells.

Keywords: Acalabrutinib · B cell · BCR signaling · Bruton's tyrosine kinase · Phosphoflow cytometry



Additional supporting information may be found online in the Supporting Information section at the end of the article.

Introduction

Bruton's tyrosine kinase (BTK) is a critical component of the BCR signaling pathway that is crucial for development, activation, and differentiation of B cells, and supports B-cell survival and progres-

sion of disease in various B-cell malignancies [1, 2]. In chronic lymphocytic leukemia (CLL) and mantle-cell lymphoma (MCL), constitutive BCR signaling promotes clonal activation and accumulation of malignant B cells [3]. Targeting BTK activity with ibrutinib, a BTK inhibitor that covalently binds Cys481 in its kinase domain, has demonstrated impressive clinical efficacy in

Correspondence: Prof. Rudi W. Hendriks and Dr. Odilia B. J. Corneth
e-mail: r.hendriks@erasmusmc.nl; o.corneth@erasmusmc.nl

[#]These authors contributed equally to this work.

CLL and MCL [4, 5]. Second-generation BTK inhibitors, such as acalabrutinib, show superior efficacy with limited toxicity and off-target side-effects [6]. Recently, a study showed that BTK inhibitors can effectively treat other B-cell-mediated diseases as treatment with evobrutinib decreased the formation of active lesions in MS patients [7].

Functional BTK protein is essential for B cells, as loss-of-function mutations in the *BTK* gene lead to the inherited immunodeficiency disease X-linked agammaglobulinemia (XLA). In these patients, B-cell development is arrested at the pre-B cell stage, leading to an almost complete absence of peripheral B cells and circulating antibodies [8, 9]. Although in Btk-deficient mice, peripheral B-cell maturation and activation is significantly affected [10–12], the B-cell developmental block in the BM is mild. However, combined deficiency of Btk and its family member Tec or the B-cell linker molecule SLP-65 results in a severe block in B-cell development [13, 14]. Using an inducible knock-out model, it was recently shown that Btk is not required for maintenance of the existing follicular B-cell pool, although B cells did not proliferate upon anti-IgM stimulation [15].

Treatment of CLL and MCL patients with ibrutinib or acalabrutinib strongly decreases disease activity [3–6, 16], but in some patients prolonged exposure to BTK inhibitors is associated with development of resistance. Therapy resistance may originate either from genetic mutations in signaling molecules, acquired changes in BCR signaling, or upregulation of compensatory pathways that provide proliferation or survival signals. In this context, patients relapsing upon inhibition therapy showed mutation of the BTK inhibitor binding site Cys481, or a gain-of-function mutation in the BTK-downstream effector PLC γ 2 [17]. Acquired mutations in various other genes, such as *MYD88*, *TP53*, *SF3B1*, and *CARD11*, were also identified. Inhibition of driver oncogene function is associated with rapid rewiring of signal transduction pathways in many tumor types [18]. This phenomenon mirrors regular feedback mechanisms in nonmalignant cells, whereby kinase activation engages homeostatic mechanisms that inactivate upstream signaling [19]. For example, a significant reduction in total BTK protein expression was observed in CLL cells from ibrutinib-treated patients or in diffuse large B-cell lymphoma lines chronically exposed to BTK-inhibition [17]. Conversely, BTK protein levels are upregulated upon stimulation of mature cells through the BCR, CD40, or TLRs [20, 21].

It remains unknown whether the observed rewiring reflects selection of tumor cells from a heterogeneous population or inhibitor-induced molecular changes, for example, by epigenetic modifications. Indeed, ibrutinib treatment was associated with substantial genome-wide changes in chromatin accessibility and histone modifications [22]. Furthermore, the effects of Btk-deficiency or long-term kinase inhibition on BCR signaling of nonleukemic mature B cells remain poorly characterized.

In this report, we aimed to explore the consequences of in vivo Btk-kinase inhibition on the phosphorylation status of key BCR signaling molecules in splenic B cells in mice. Remarkably, Btk-deficiency and prolonged in vivo acalabrutinib treatment was associated with increased proximal BCR signaling and divergent

downstream signaling in follicular B cells, but not in transitional and marginal zone (MZ) B cells. These findings provide evidence that BTK inhibition induces complex rewiring of BCR signaling.

Results

Btk-deficient B cells show aberrant anti-IgM-induced activation of distal BCR signaling proteins

First, we aimed to confirm that Btk is crucial for BCR signaling and compared unstimulated and anti-IgM-stimulated splenic B220⁺CD21⁻CD23⁺ follicular B cells from Btk-deficient (*Btk*^{-/-}) and WT mice (for gating strategy: see Supporting information Fig. S1). The main BCR downstream pathways, Akt, NF- κ B, PLC γ 2, and MAPK, were analyzed by flow cytometry.

We first quantified S240/244 phosphorylation of the ribosomal protein S6 as a measure of activation of the Akt pathway. No differences were detected between unstimulated *Btk*^{-/-} and WT follicular B cells, but *Btk*^{-/-} follicular B cells displayed increased S6 phosphorylation after 30 min and decreased S6 phosphorylation after 120–360 min of anti-IgM stimulation, compared with WT B cells (Fig. 1A). Accordingly, in vitro culture of splenic B cells with acalabrutinib showed that S6 phosphorylation at 120–180 min was highly dependent on Btk kinase activity (Supporting information Fig. S2A).

As expected [23, 24], anti-IgM-driven NF- κ B activation was decreased in *Btk*^{-/-} follicular B cells, as evidenced by reduced degradation of the inhibitory protein I κ B α and reduced expression of c-Rel protein (Fig. 1B). Although Ca²⁺ influx was reduced upon anti-IgM stimulation, phosphorylation of the key Btk-effector PLC γ 2 (Y759) was increased in *Btk*^{-/-} B cells, compared with WT B cells (Fig. 1C). Strikingly, anti-IgM-induced pErk (T202/Y204) was significantly higher in *Btk*^{-/-} B cells than in WT B cells (Fig. 1D).

In line with the strongly reduced activation of the Akt/S6 and NF- κ B pathways, the induction of the antiapoptotic proteins Mcl-1 and Bcl-XL by these two pathways, respectively [25, 26], was significantly impaired in *Btk*^{-/-} follicular B cells upon 22 h stimulation with anti-IgM (Fig. 1E).

Taken together, these findings indicate that Btk-deficiency differentially affected the main distal BCR signaling pathways. Whereas NF- κ B and Akt signaling was hampered, pErk and pPLC γ 2 expression was remarkably increased in anti-IgM-stimulated *Btk*^{-/-} B cells.

Btk-deficient B cells show increased phosphorylation of proximal BCR signaling molecules

To more comprehensively study the effects of Btk-deficiency, we investigated phosphorylation of key BCR proximal signaling molecules in splenic follicular B cells. Upon BCR engagement, the signaling cascade starts with phosphorylation of a Src-family kinase, most probably Lyn. Both at the activating

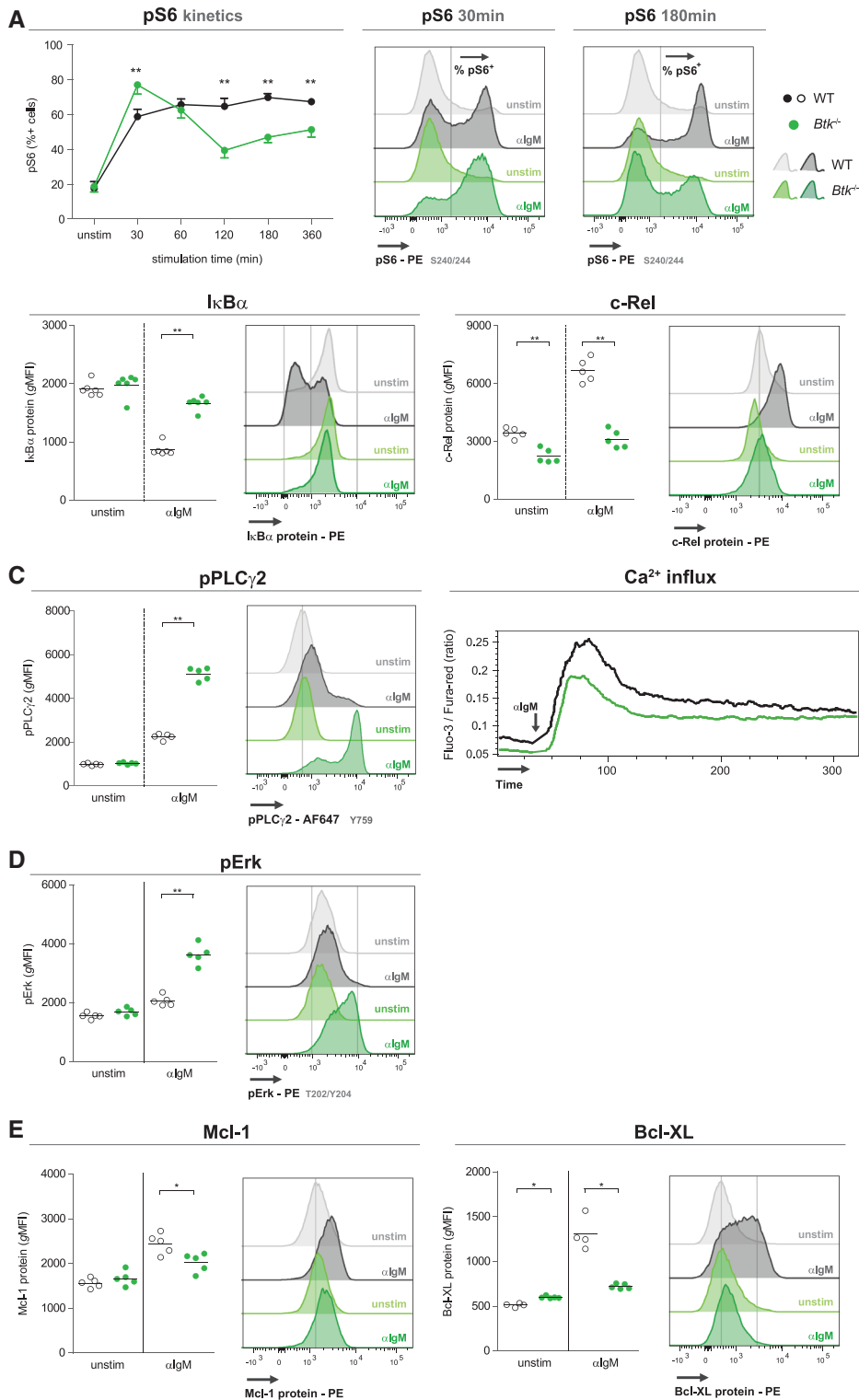


Figure 1. BCR signaling is rewired in *Btk*-deficient follicular B cells. (A) Ribosomal protein S6 phosphorylation kinetics represented by percentage of positive cells in follicular splenic B cells after 30, 60, 120, 180, and 360 min incubation with anti-IgM stimulation. (B) Quantification by geometric mean fluorescence intensity (gMFI) for IκBα protein degradation after 1 h and c-Rel protein degradation after 22 h of anti-IgM stimulation of follicular splenic B cells. (C) gMFI for pPLCγ2 after 5 min of anti-IgM stimulation (left) and Ca²⁺ influx measurement (right) in B220⁺ B cells upon stimulation with 25 μg anti-IgM in WT and *Btk*^{-/-} mice, representative for five mice analyzed. (D) gMFI for Erk phosphorylation after 5 min of anti-IgM stimulation. (E) Quantification by gMFI for Mcl-1 and Bcl-XL after 22 h of anti-IgM stimulation. Representative histogram overlays are depicted on the right of all panels. All data were measured by flow cytometry. Symbols represent individual mice and lines indicate mean values. Graphs represent three to four individual experiments, each graph with 5–6 mice per group. *Btk*-deficient (*Btk*^{-/-}) mice and WT controls were 8–12 weeks old; **p* < 0.05, ***p* < 0.01 by Mann–Whitney U test.

Y424 and the inhibitory Y507 site [27], Src phosphorylation was slightly reduced in unstimulated *Btk*^{-/-} follicular B cells. Very surprisingly, phosphorylation at both pSrc sites was significantly increased upon anti-IgM stimulation in *Btk*^{-/-} follicular B cells compared with WT controls (Fig. 2A; Supporting information Fig. S2B).

While basal pCD79a (Y182) was only slightly increased in *Btk*^{-/-} follicular B cells, the level of anti-IgM-induced pCD79a was remarkably higher in *Btk*^{-/-} B cells than in WT B cells (Fig. 2B). This phenomenon was not due to high CD79a protein expression in *Btk*^{-/-} follicular B cells. On the contrary, in *Btk*^{-/-} follicular B cells CD79a expression was somewhat lower,

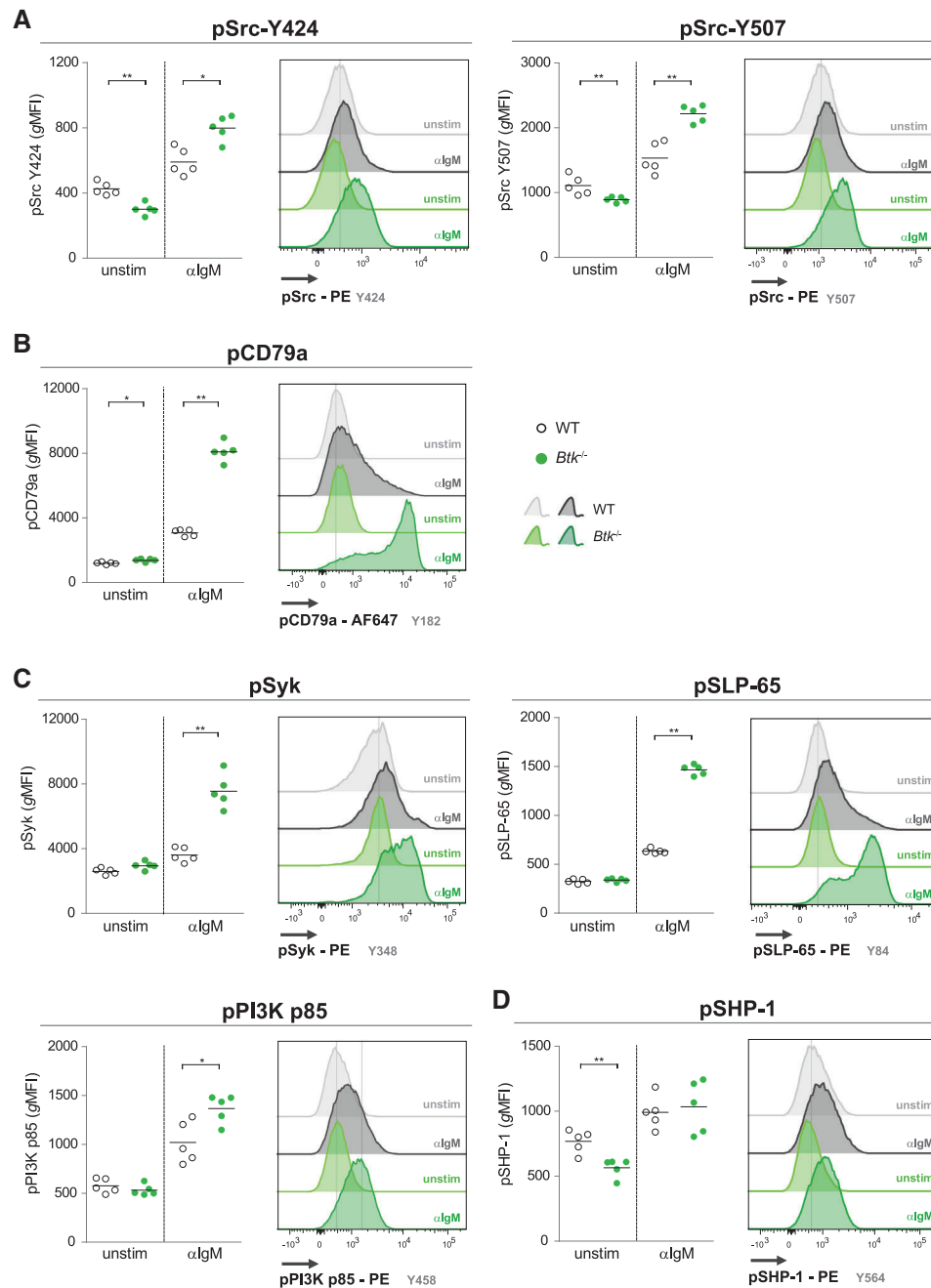


Figure 2. Proximal BCR signaling is strongly increased in *Btk*-deficient follicular B cells. (A) Quantification by geometric mean fluorescence intensity (gMFI) for either 5 min for pSrc-Y424 or pSrc-Y507 of anti-IgM stimulation and gated for follicular B cells. (B) Quantification gMFI for pCD79a after 5 min of anti-IgM stimulation in *Btk*^{-/-} follicular B cells compared to WT counterparts. (C-D) Quantification (gMFI) after 5 min of anti-IgM stimulation for (C) pSyk and pSLP-65, 1 min for pPI3K p85 and (D) 3 min for pSHP-1 in follicular B cells. Representative histogram overlays are depicted on the right. All data were measured by flow cytometry. Symbols represent individual mice and lines indicate mean values. Graphs represent three to four individual experiments, each graph with 4–6 mice per group; *Btk*-deficient (*Btk*^{-/-}) mice and WT controls were 8–12 weeks old; **p* < 0.05, ***p* < 0.01 by Mann–Whitney *U* test.

yet CD79b expression was higher than in WT B cells (Supporting information Fig. S3A).

Like pCD79a, also anti-IgM-induced phosphorylation of Syk (Y348), SLP-65 (Y84), and the p85 PI3K subunit (Y458) was significantly increased in *Btk*^{-/-} follicular B cells (Fig. 2C).

Protein levels of Syk and PLCγ2, however, were decreased or unchanged in *Btk*^{-/-} follicular B cells (Supporting information Fig. S3A). Unstimulated *Btk*^{-/-} follicular B cells displayed reduced phosphorylation of SHP-1 at Y564, a phosphatase with the capacity to dephosphorylate BCR downstream targets and are

recruited by inhibitory receptors such as CD5, CD22, and Siglec-G [28–30]. Upon anti-IgM stimulation, however, pSHP-1 was similar in *Btk*^{-/-} and WT follicular B cells (Fig. 2D), indicating that the increased anti-IgM-induced phosphorylation of proximal BCR signaling molecules in *Btk*^{-/-} B cells cannot be explained by reduced SHP-1 phosphatase activity.

In summary, anti-IgM-induced phosphorylation of key proximal BCR signaling molecules was significantly higher in *Btk*-deficient than in WT follicular B cells, indicating that the absence of *Btk* is associated with rewiring of BCR signaling.

Limited BCR rewiring in *Btk*-deficient splenic transitional and MZ B cells

As we previously found differences in basal PLC γ 2 phosphorylation across transitional, follicular and MZ B cells in the spleen of WT mice [31], we next investigated basal phosphorylation and BCR signaling responsiveness in WT mice in these three splenic B-cell subpopulations. Compared to follicular B cells, basal phosphorylation of CD79a, Syk, PLC γ 2, Erk, and S6 was similar or only slightly higher in T1 transitional B cells (Fig. 3A; see for gating: Supporting information Fig. S1). However, upon BCR stimulation transitional T1 B cells showed an enhanced responsiveness to BCR engagement compared to follicular B cells for CD79a, Syk, PLC γ 2, and Erk, whereas anti-IgM-induced pS6 was reduced (Fig. 3A). In contrast, in MZ B-cell basal phosphorylation of Syk, PLC γ 2, Erk, and S6 was significantly increased, compared to follicular B cells. Upon BCR stimulation, MZ B cells exhibited increased phosphorylation of CD79a, Syk, PLC γ 2, and Erk when compared with follicular B cells (Fig. 3A). However, the proportions of pS6-positive cells following anti-IgM stimulation were comparable between MZ and follicular B cells (Fig. 3A). Essentially, these findings imply that—except for pS6—T1 transitional B cells are more responsive to BCR signaling and that MZ B cells show a preactivated basal signaling, when compared to follicular B cells.

Next, we investigated whether BCR signaling was altered in *Btk*^{-/-} T1 and MZ B cells. Whereas we observed limited differences between *Btk*^{-/-} and WT T1 B cells in basal phosphorylation of CD79a, Syk, and Erk, phosphorylation of Src-Y424, Src-Y507, PLC γ 2, and S6 was significantly lower in *Btk*^{-/-} T1 B cells (Fig. 3B). BCR stimulation of *Btk*^{-/-} T1 B cells resulted in higher pCD79a, similar to pSrc-Y424, pSrc-Y507, pSyk, pPLC γ 2, and pErk, and reduced pS6, compared with WT T1 B cells.

In *Btk*^{-/-} MZ B cells, basal phosphorylation of all signaling molecules was significantly lower than in WT MZ B cells, except for Syk (Fig. 3B). Differences were generally moderate, but considerable for pSrc-Y424, pSrc-Y507, and pS6. BCR stimulation of *Btk*^{-/-} MZ B cells resulted in significantly higher pCD79a, similar to pSrc-Y424, pSrc-Y507, pSyk, pPLC γ 2, and pErk, and reduced pS6, compared with WT MZ B cells, paralleling our findings in T1 B cells.

Taken together, we observed complex BCR signaling differences across different splenic B-cell subpopulations. Compared with *Btk*-deficient follicular B cells both splenic transitional and

MZ B cells showed only limited BCR rewiring, characterized by modestly increased pCD79a and decreased pS6.

Enhanced upstream BCR signaling in *Btk*^{-/-} B cells is independent of differences in IgM/IgD profile

As *Btk*-deficient B cells have increased IgM expression and fail to fully upregulate IgD [10, 32, 33], we investigated whether an altered IgM/IgD expression profile contributed to the strong increase in proximal signaling in *Btk*^{-/-} B cells. To compare follicular B cells with similar BCR expression levels between *Btk*^{-/-} and WT mice, we gated for nine different populations (P1–9) with variable expression for IgD and Ig κ/λ light chain (Fig. 4A).

All nine gated populations showed higher CD79a phosphorylation in anti-IgM-stimulated *Btk*^{-/-} B cells than in WT B cells, showing that increased pCD79a in *Btk*^{-/-} follicular B cells is independent of the IgM/IgD profile (Fig. 4B). Increasing Ig κ/λ expression, while retaining similar IgD expression resulted in increased pCD79a signaling of WT B cells and even more so in *Btk*^{-/-} follicular B cells (most evident in the P7–P8–P9 comparison). The IgM/IgD expression profile (with similar total Ig surface expression, inferred from Ig κ/λ signals) appeared to control the magnitude of the pCD79a response in *Btk*^{-/-} B cells: pCD79a expression further increased in *Btk*^{-/-} but not in WT follicular B cells with lower IgD expression values, for example, in a P2–P5–P8 comparison (Fig. 4B and C). Similar results were found for pPLC γ 2 (Fig. 4D and E). Last, we stimulated B cells with F(ab')₂-Ig κ light chain fragments to check whether signaling is increased in *Btk*^{-/-} B cells when stimulating both the IgD and IgM BCR and found that this was indeed the case (Fig. 4F).

Collectively, these data show that IgM and IgD expression differences between *Btk*^{-/-} and WT B cells cannot explain the increased BCR responsiveness and rewiring in *Btk*^{-/-} follicular B cells.

Proximal BCR signaling is enhanced in follicular B cells overexpressing *Btk*

Given that *Btk*-deficiency strongly affected phosphorylation of both proximal and distal BCR signaling molecules, we investigated whether overexpression of *Btk* protein had opposite effects. Indeed, when we analyzed B cells from CD19-h*Btk* transgenic mice with B-cell-specific overexpression of human BTK, we found that CD79a phosphorylation was significantly decreased both in unstimulated and anti-IgM stimulated follicular B cells (Fig. 5A). Also, a trend of decreased BCR responsiveness to anti-IgM stimulation was observed by calculating the ratio geometric mean fluorescence intensity (gMFI) between stimulated and unstimulated follicular B cells for pPLC γ 2 and p*Btk*, although this was not significant (Fig. 5B and C). This could not be explained by decreased protein levels, because expression of CD79a was only slightly reduced and levels of other BCR signaling protein, including pPLC γ 2, were essentially unchanged compared to WT B

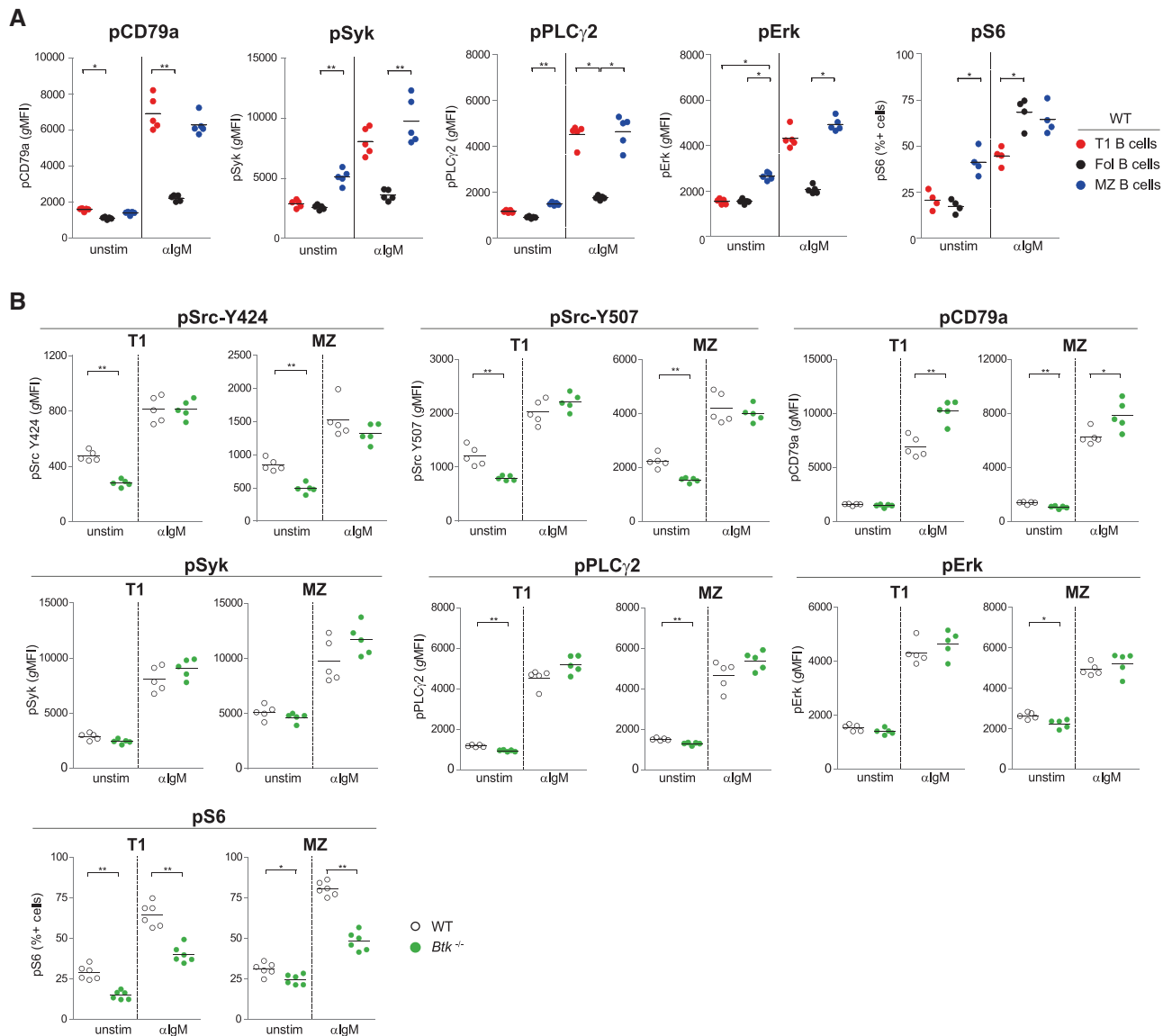


Figure 3. Limited rewiring of BCR signaling in Btk-deficient marginal zone and transitional type 1 B cells. (A) Quantification by geometric mean fluorescence intensity (gMFI) after 5 min of anti-IgM stimulation for pCD79a, pSyk, pPLC γ 2 and pErk or by percentage of positive cells after 3 h stimulation with anti-IgM for pS6 in transitional type 1 (T1), marginal zone (MZ) and follicular (Fol) B cells from WT mice. (B) Quantification by gMFI after 5 min of anti-IgM stimulation for pSrc-Y424, pSrc-Y507, pCD79a, pSyk, pPLC γ 2, and pErk or by percentage of positive cells after 3 h stimulation with anti-IgM for pS6 in T1 and MZ B cells from the indicated mice. All data were measured by flow cytometry. Symbols represent individual mice and lines indicate mean values. Graphs represent two to three individual experiments, each graph with 4–6 mice per group; Btk-deficient (*Btk*^{-/-}) mice and WT controls were 8–12 weeks old; **p* < 0.05, ***p* < 0.01 by Kruskal–Wallis with Dunn’s multiple comparison posthoc test (A) or Mann–Whitney *U* test (B).

cells (Supporting information Fig. S3B). Also, CD19-hBtk follicular B cells showed increased pErk in unstimulated and anti-IgM-stimulated B cells, whereby BCR responsiveness was comparable to WT counterparts (Fig. 5D).

Other distal signaling pathways did show the expected pattern: in CD19-hBtk B cells anti-IgM-induced NF- κ B activation was enhanced, since I κ B α degradation was increased (Fig. 5E). As previously reported [34], anti-IgM-induced activation of the Akt/S6 signaling pathway was enhanced (Fig. 5F).

Taken together, these findings show that increased Btk expression and Btk-deficiency had essentially opposite effects on BCR signaling, perhaps with the exception of Erk phosphorylation.

Single-dose in vivo Btk inhibition mainly affects distal BCR signaling molecules

Next, we aimed to study whether inhibition of Btk kinase activity would cause similar rewiring of BCR signaling as

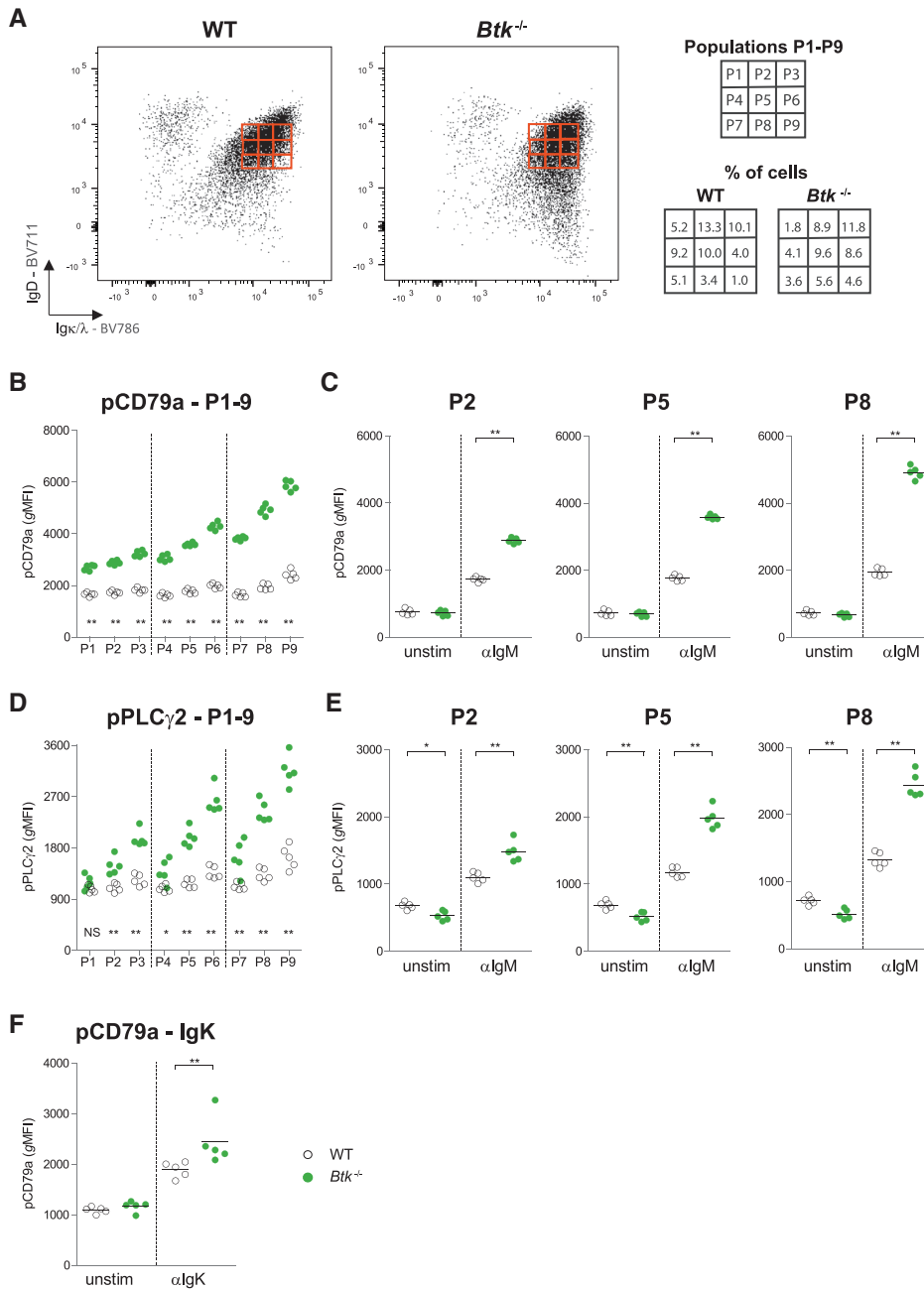


Figure 4. Enhanced upstream BCR signaling in *Btk*-deficient B cells is independent of differences in IgM/IgD profile. (A) Gating strategy for nine populations (P1–P9) differing in BCR expression based on IgD and light chain expression levels. The expression of IgD and the light chain measured by geometric mean fluorescence intensity (gMFI) was similar between *Btk*-deficient (*Btk*^{-/-}) and WT follicular B cells in these nine gated populations. (B–C) Quantification by gMFI after 5 min of anti-IgM stimulation for pCD79a (B–C) and pPLCγ2 (D–E), showing P1–9 for both *Btk*^{-/-} and WT follicular B cells in one graph (B,D) or specifically P2, P5 and P8 including unstimulated controls (C,E). (F) Quantification by gMFI after 5 min of anti- κ light chain (anti-IgK) stimulation for pCD79a. All data were measured by flow cytometry. Graphs represent two to three individual experiments, each graph with five mice per group; Symbols represent individual mice and lines indicate mean values; *Btk*^{-/-} and WT mice were 8–12 weeks of age; **p* < 0.05, ***p* < 0.01 by Mann–Whitney U test.

observed in *Btk*^{-/-} follicular B cells. We treated WT mice in vivo with acalabrutinib or vehicle control by oral gavage. After 3 h of treatment, anti-IgM-induced calcium signaling was strongly decreased in follicular B cells from acalabrutinib-treated mice compared with these cells from vehicle-treated control mice (Fig. 6A). The proximal signaling molecules analyzed essentially showed somewhat decreased basal signaling in follicular B cells after acalabrutinib treatment (Fig. 6B). Upon anti-IgM stimulation, phosphorylation of CD79a was significantly decreased in follicular B cells from acalabrutinib-treated mice, but other proximal signaling molecules retained similar levels of anti-IgM-induced phosphory-

lation, compared to follicular B cells from vehicle-treated mice (Fig. 6B).

By contrast, analysis of distal BCR signaling molecules revealed that Erk and pS6 phosphorylation and $\text{I}\kappa\text{B}\alpha$ degradation were significantly reduced in anti-IgM-stimulated B cells from acalabrutinib-treated mice, compared with control mice (Fig. 6C).

In conclusion, in vivo acalabrutinib administration strongly affected distal mediators of the BCR signaling cascade within 3 h, as expected. Moreover, *Btk* inhibition had subtle upstream effects, particularly resulting in reduced phosphorylation of the very proximal CD79a BCR signaling molecule.

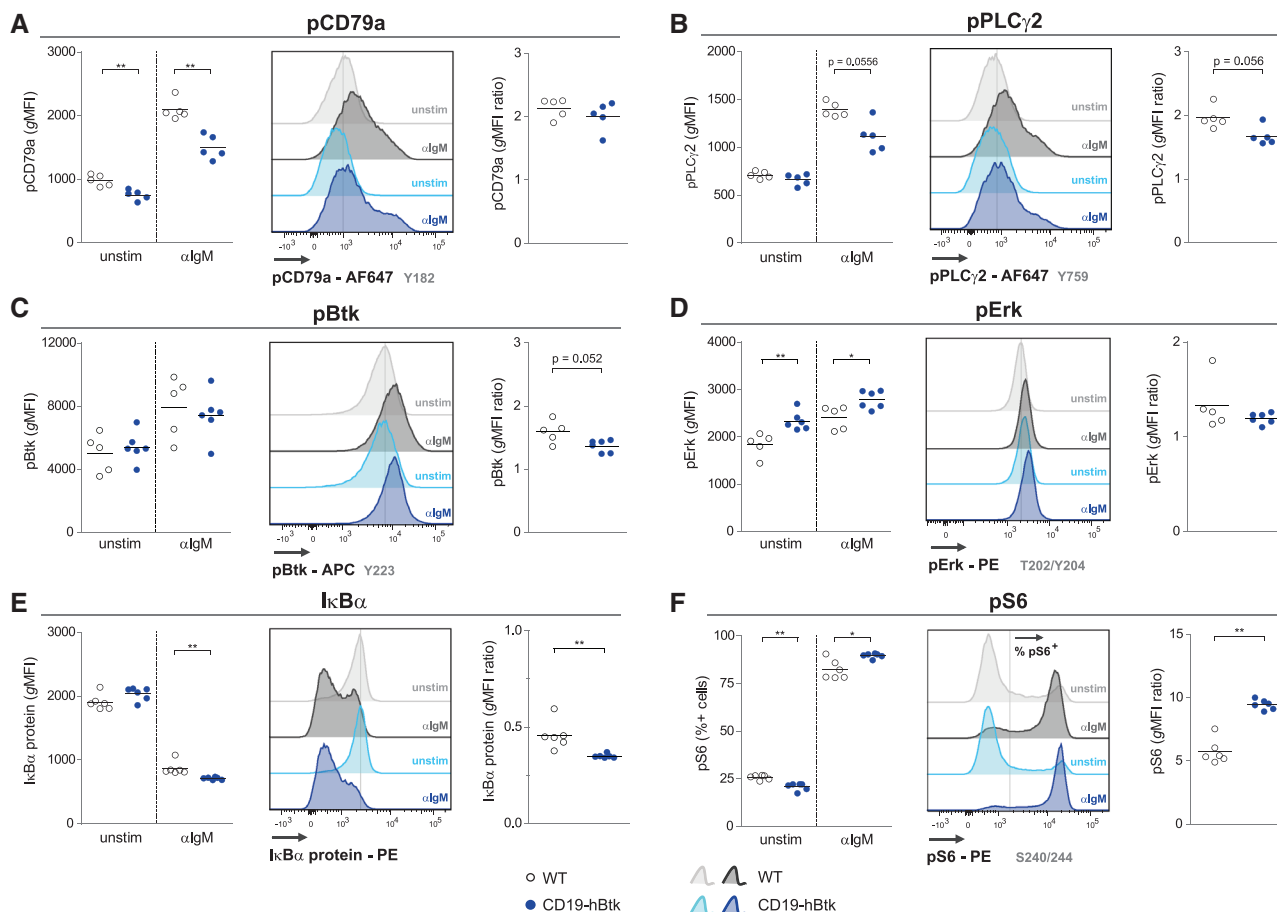


Figure 5. Decreased proximal signaling in CD19-hBtk follicular B cells. (A–F) Splenic cells of CD19-hBtk Btk-overexpressing mice and WT controls were stimulated for either 5 min for pCD79a (A), pPLCγ2 (B), pBtk (C), and pErk (D), 1 h for IκBα (E) or 3 h for pS6 (F) and gated for follicular B cells after the indicated in vitro stimulation with anti-IgM. All panels show quantification by geometric mean fluorescence intensity (gMFI) (A–E) or by percentage of positive cells (pS6; F) (left), a histogram overlay of representative samples (middle) and stimulation ratio calculated by fold increase in anti-IgM-stimulated gMFI compared to unstimulated counterparts (right). All data were measured by flow cytometry. Symbols represent individual mice and lines indicate mean values. Graphs represent two to three individual experiments, each graph with five mice per group; CD19-hBtk and WT mice were 8–12 weeks old; *p < 0.05, **p < 0.01 by Mann–Whitney U test.

Prolonged in vivo Btk inhibition mimics rewiring of BCR signaling as observed in Btk-deficient mice

Next, we treated WT mice with acalabrutinib or vehicle in drinking water for 5 days, to investigate rewiring following prolonged kinase inhibition.

Compared to B cells from vehicle-treated mice, calcium influx following anti-IgM stimulation was decreased in B cells from acalabrutinib-treated mice and similar to *Btk*^{-/-} B cells (Fig. 7A). Follicular B cells from acalabrutinib-treated mice showed increased IgM and similar IgD expression, reminiscent of the IgM/IgD profile of B cells in *Btk*^{-/-} mice, while expression of CD79b was increased and Btk protein was decreased (Supporting information Fig. S4A). Phosphorylation of CD79a and PLCγ2 was increased upon stimulation with anti-IgM in acalabrutinib-treated follicular B cells compared to vehicle-treated counterparts (Fig. 7B and C). We also observed increased BCR responsiveness of acalabrutinib-treated follicular B cells for pSrc-Y424 and

pSrc-Y507 (Fig. 5D), although this was mainly due to the decreased basal signaling (Supporting information Fig. S4B).

Prolonged acalabrutinib treatment strongly affected distal BCR signaling: IκBα degradation and phosphorylation of Akt and S6 were significantly reduced (Supporting information Fig. S4C and D). Acalabrutinib treatment reduced basal Erk signaling, but the anti-IgM-induced phosphorylation was similar, resulting in increased BCR responsiveness for pErk (Supporting information Fig. 4E).

Finally, we investigated whether BCR rewiring is also induced upon Btk inhibition in malignant B cells, we employed a chronic lymphocyte leukemia (CLL) mouse model. We transferred EMC6 CLL cells, derived from the *IgH.TEμ* mice that spontaneously develop CLL [35, 36] intraperitoneally into *Rag1*^{-/-} mice (Fig. 7E). After 12 days, we detected circulating IgM⁺CD5⁺ CLL cells confirming EMC6 engraftment in these *Rag1*^{-/-} mice, in line with published findings [36]. To study the effect of in vivo Btk inhibition in CLL cells, we treated the mice with the Btk-inhibitor

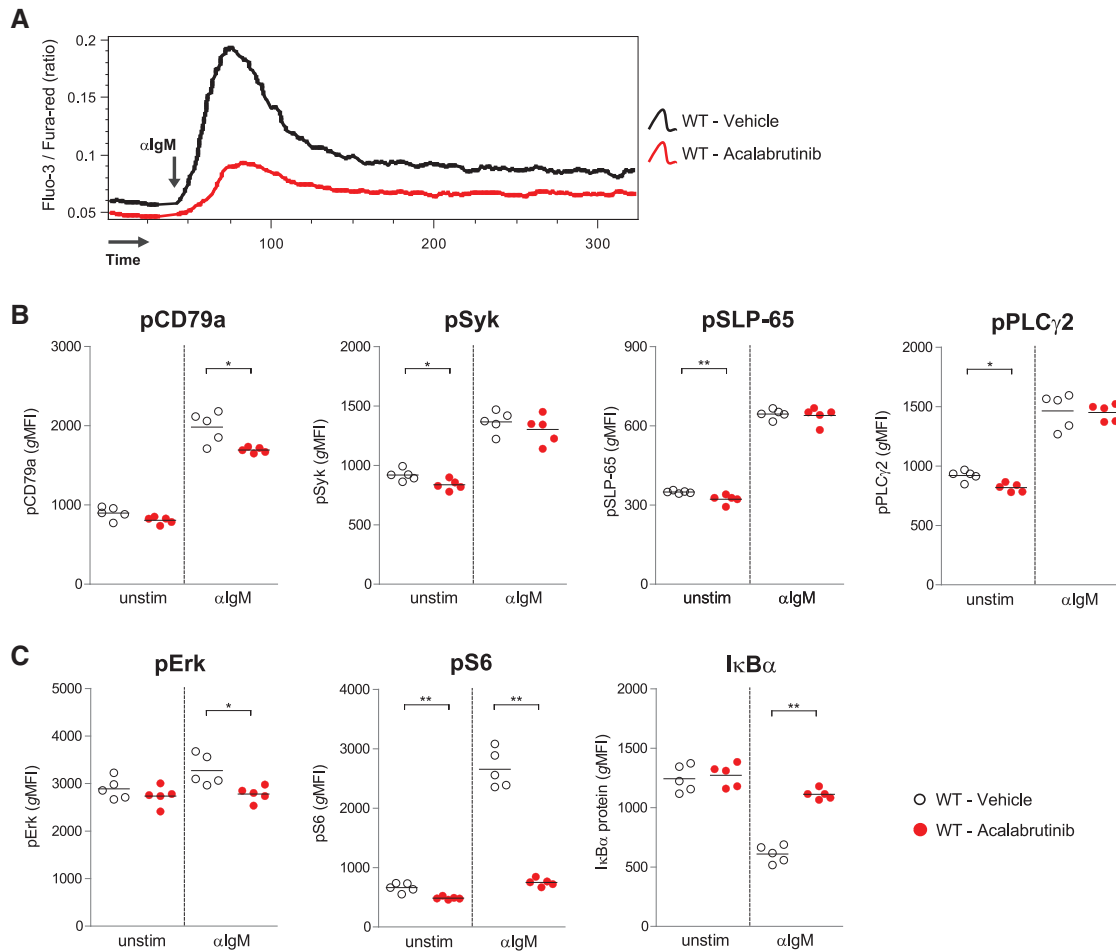


Figure 6. Single-dose in vivo Btk-kinase inhibition affects basal phosphorylation of proximal BCR molecules. CBA/J mice were treated in vivo by administration of one single dose of acalabrutinib or vehicle control by oral gavage. (A) Ca^{2+} influx measurement in B220^{+} B cells upon stimulation with $25 \mu\text{g}$ anti-IgM in vehicle or acalabrutinib-treated mice, representative for five mice analyzed. (B) Quantification by geometric mean fluorescence intensity (gMFI) for pCD79a, pSyk, pSLP-65, and pPLC γ 2 after 5 min stimulation of anti-IgM. (C) Quantification by gMFI for pErk after 5 min, for $\text{I}\kappa\text{B}\alpha$ protein after 1 h, and pS6 after 180 min of anti-IgM stimulation of follicular B cells. All data were measured by flow cytometry. Graphs represent two individual experiments, each graph with 4–5 mice per group. Symbols represent individual mice and lines indicate mean values; each group contained five 12-week-old CBA/J WT mice; * $p < 0.05$, ** $p < 0.01$ by Mann–Whitney U test.

ibrutinib, or vehicle as a control, for a maximum of 14 days (Fig. 7E). Treatment with ibrutinib significantly enhanced the survival as compared to vehicle-treated mice (Fig. 7F), with two ibrutinib-treated mice reaching the experimental end-point of 20 days after start of treatment. We analyzed spleens of end-stage CLL mice, implying that for ibrutinib-treated mice the analysis was performed approximately 3 to 5 days after the end of 14-day treatment. In line with findings in acalabrutinib-treated WT B cells, the engrafted EMC6 CLL cells showed significantly enhanced upstream BCR signaling compared to WT controls, as evidenced by increased phosphorylation of CD79a, Syk, SLP-65, and PLC γ 2 (Fig. 7G). The increased phosphorylation could not be explained by increased total protein levels of these signaling molecules (Supporting information Fig. S5A and B).

Taken together, these data show that prolonged in vivo Btk inhibition results in rewiring of BCR signaling pathways, both upstream and downstream of Btk, in follicular B cells, paralleling

our findings in Btk-deficient mice. Moreover, in vivo Btk inhibition was also associated with a similar rewiring of BCR signaling in leukemic B cells.

Discussion

Btk protein is a crucial BCR signaling protein and tight regulation of expression levels and kinase activity are important for normal B-cell development and function. Btk inhibition is a successful treatment for several B-cell malignancies, but its (long-term) effects on signaling have not been assessed. Our findings implicate that Btk inhibition may have more far-reaching effects than previously anticipated. In addition to downstream signaling routes, Btk inhibition also affects proximal upstream BCR signaling and rewires the entire BCR signaling cascade.

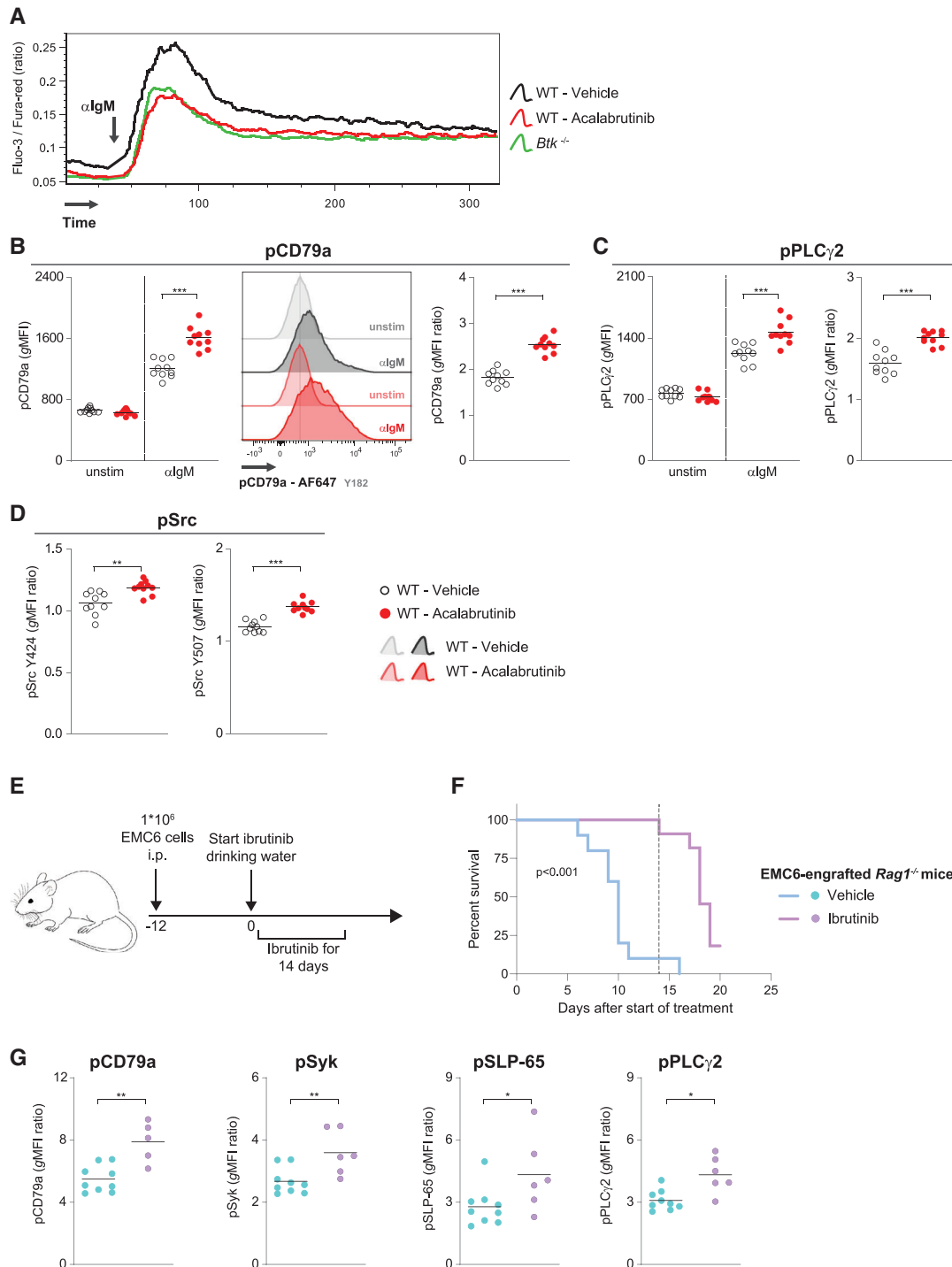


Figure 7. Prolonged Btk-kinase inhibition in vivo leads to enhanced proximal signaling. CBA/J mice were treated in vivo with drinking water containing acalabrutinib or vehicle control for 5 days. (A) Ca²⁺ influx measurement of B220⁺ B cells upon stimulation with 25 μ g anti-IgM in vehicle or acalabrutinib-treated CBA/J mice compared to untreated Btk-deficient (*Btk*^{-/-}) mice. (B) Quantification by geometric mean fluorescence intensity (gMFI) in follicular B cells after 5 min for pCD79a (left), representative histogram overlay (middle), and stimulation ratio calculated by fold increase in anti-IgM-stimulated gMFI compared to unstimulated counterparts (right). (C) Quantification by gMFI (left) and stimulation ratio (calculated by fold increase in anti-IgM-stimulated gMFI compared to unstimulated counterparts; right) of pPLC γ 2 after 5 min of anti-IgM stimulation. (D) Stimulation ratios for pSrc-Y424 and pSrc-Y507. (E) Experimental design for EMC6-engraftment and ibrutinib treatment of *Rag1*^{-/-} mice (F) Retrospective Kaplan–Meier incidence curve depicting survival of EMC6-engrafted *Rag1*^{-/-} mice treated with ibrutinib or vehicle drinking water, n = 11 mice per group, data from two experiments. Dotted grey line indicates stop of ibrutinib treatment at day 14 (G) Quantification of the stimulation ratio for pCD79a, pSyk, pSLP-65, and pPLC γ 2 after 5 min of anti-IgM stimulation in EMC6-engrafted *Rag1*^{-/-} mice. All data were measured by flow cytometry (except for panel E and F). Graphs represent two individual experiments, each graph with 4–11 mice per group; CBA/J WT, *Btk*^{-/-} mice and *Rag1*^{-/-} mice were 8–12 weeks old. Symbols represent individual mice and lines indicate mean values; **p* < 0.05, ***p* < 0.01, ****p* < 0.001 by Mann–Whitney U test.

Downstream signaling by NF- κ B and Akt was shown to be critically dependent on Btk protein [23, 24, 37]. Conversely, we previously showed that Akt signaling is enhanced in Btk-overexpressing B cells upon BCR stimulation [34]. In vitro blockade of Btk-kinase activity leads to decreased basal signaling of Akt, NF- κ B, and ERK in B cells from CLL patients and mouse models [36, 38, 39]. Decreased basal downstream signaling was also observed after 1–4 weeks in vivo acalabrutinib treatment in a TCL-1 adoptive transfer CLL model [39], however, BCR responsiveness or proximal signaling were not investigated. Here, we also observed effects on basal signaling in nontransformed B cells, however, the most apparent difference was the strongly decreased response to BCR stimulation upon in vivo acalabrutinib treatment.

Btk-deficient and X-chromosome-linked immunodeficiency mice show decreased calcium signaling upon BCR stimulation [40, 41]. While basal calcium is unchanged in CD19-hBtk B cells, anti-IgM-induced calcium influx is enhanced in CD19-hBtk B cells [42]. A very recent study showed that B cells with strongly impaired calcium influx capacity show altered pS6 kinetics, resulting in an earlier pS6 peak and a decreased capacity to induce other downstream mediators including Myc and IRF4 [43]. This is similar to our findings in *Btk*^{-/-} follicular B cells, which showed increased pS6 at 30 min but decreased pS6 at 180 min of anti-IgM stimulation compared to WT controls. It is, therefore, likely that Btk-dependent calcium signaling alters pS6 signaling kinetics, and may thereby impact B-cell survival.

Interestingly, anti-IgM-induced pErk was markedly increased specifically in follicular B cells from *Btk*^{-/-} and acalabrutinib-treated mice, compared to untreated WT mice. Because Erk was shown to be crucial for survival and differentiation of immature B cells in a mouse strain with low-surface BCR levels [44], it is conceivable that enhanced Erk signaling is advantageous for *Btk*^{-/-} follicular B cells. Further experiments are required to investigate why this is not the case for T1 or MZ B cells in *Btk*^{-/-} mice, in which Erk signaling is comparable to WT mice.

Very surprisingly, we found that Btk activity dictated the signaling of proximal BCR signaling molecules in follicular B cells. While Btk inhibition significantly reduced anti-IgM-mediated CD79a phosphorylation within 3 h of in vivo acalabrutinib treatment, genetic Btk-deficiency, or prolonged acalabrutinib treatment increased BCR responsiveness for the entire proximal signaling hub. Our findings are in concordance with the reported increased BCR-induced pCD79a and pSyk in *Btk*^{-/-} mice [45]. In this study, in vitro inhibition by ibrutinib resulted in reduced pSyk, even in *Btk*^{-/-} B cells [45], indicating an off-target effect of ibrutinib. Very recently, BCR rewiring was also reported in a mouse model with B-cell specific deletion of TNF receptor associated factor 3 (TRAF3); TRAF3-deficient B cells showed increased BCR responsiveness in upstream signaling molecules, enhanced calcium influx, and pErk signaling upon BCR stimulation [46]. This is similar to our findings, although we did not observe increased calcium signaling. This could either relate to calcium being a quite direct downstream of target of Btk, or that increased phosphatase signaling downregulates the calcium response. Likewise, it cannot formally be excluded that off-target effects contributed to BCR-

induced kinome fingerprint changes in samples from CLL patients before and after ibrutinib treatment [47]. The observed marked increase in the BCR-induced kinome signature might be related to increased surface IgM expression in patients receiving therapy. However, our analyses in Btk-deficient mice (Fig. 4) indicated that enhanced signaling was observed irrespectively of the differences in IgM/IgD profile which controls B-cell responsiveness [48, 49]—between *Btk*^{-/-} and WT B cells.

The mechanisms by which Btk controls upstream signaling remain elusive, particularly because Btk differentially affects proximal signaling in follicular, T1, and MZ B cells. Several findings, for example, for CD79a, indicate that the mechanisms involved are even remarkably complex. First, acalabrutinib can both reduce and increase anti-IgM-induced pCD79a (after 3 h and after 5 days of in vivo treatment, respectively). Second, both Btk-deficiency and Btk-overexpression reduce CD79a protein levels in B cells. Third, signaling in *Btk*^{-/-} follicular B cells could be enhanced due to increased availability of CD79b molecules for IgM. However, the interpretation of these findings is complicated, because of the concomitant decrease in CD79a, which (i) is the limiting component during BCR assembly in the ER [50] and (ii) involved as homodimer in CD19 signaling B cells [51]. In addition, while our approach provides evidence for extensive rewiring, caution should be taken when interpreting data, because of the presence of multiple—activating or inhibiting—phosphorylation sites on signaling molecules, only some of which can be analyzed by available phospho-specific antibodies. Given that Btk activity regulates many crucial transcription regulators in B cells, including NF- κ B, NFAT, Fos/Jun [52, 53], it is likely that Btk inhibition does not only rewire BCR signaling by direct phosphorylation of signaling molecules but also by regulating their transcription. Since, we found that rewiring events in vivo takes a couple of days, it is to be expected that BTK does not only act directly as a kinase (and may activate phosphatases), but also indirectly regulates transcription of signaling molecules or their regulators. This would be supported by the recently reported epigenetic changes induced during ibrutinib therapy [22], as well as our transcriptome comparison of Btk-overexpressing and WT B cells, showing differential expression of many kinases, phosphatases, as well as transcription regulators [J.R., R.W.H., unpublished findings].

Our findings may have implications for the treatment of autoimmune and malignant diseases, although it is currently unknown whether BTK inhibition in human B cells is also associated with BCR rewiring. In B-cell malignancies, potential rewiring may be dampened by sequential or combination therapies of BTK inhibitors with the Bcl-2 inhibitor venetoclax [54, 55] or potentially PI3K inhibitor idelalisib. However, BCR signaling modulation by Btk inhibition is also relevant for other B-cell-mediated diseases, because Btk inhibitors were effective in numerous autoimmune mouse models [56, 57] and MS patients [7] and are currently tested in clinical trials for autoimmune disease and coronavirus disease 2019 (COVID-19) inflammation [2, 58]. In-depth analysis of BCR responsiveness and activation of B cells from autoimmune or COVID-19 patients following Btk inhibition

should show how nonmalignant B cells respond to ibrutinib therapy.

For inflammatory diseases, the consequences of BCR rewiring will likely be very different, because therapeutic intervention is not aimed at depletion of malignant B cells, but rather at regulation of B-cell function. Nevertheless, inferred from our findings in mice that BTK inhibition induces rewiring of both distal and proximal BCR signaling, in leukemic patients also signaling responsiveness of healthy B cells will be substantially altered. Therefore, it will be valuable to include a detailed analysis of BCR signaling, in future clinical trials of Btk inhibitors both in B-cell malignancies and in autoimmune disease.

Materials and methods

Mice and genotyping

Btk-deficient (*Btk*^{-/-}) [33], CD19-hBtk [59], and Rag1-deficient (*Rag1*^{-/-}) were on the C57BL/6 background [60] mice were genotyped by PCR. Nontransgenic littermates or C57/BL6 mice (Charles River, Wilmington, MA, USA) were used as WT controls. For in vivo Btk-kinase inhibition experiments, we used WT CBA/J mice (Janvier, Le Genest-Saint-Isle, France). Mice were bred and kept under specified pathogen-free conditions in the Erasmus MC experimental animal facility. All experimental protocols were reviewed and approved by the Erasmus MC Committee for animal experiments (DEC).

Flow cytometry and calcium influx

Splenic cell suspensions were prepared in RPMI 1640 supplemented with 2% FCS (RPMI-2% FCS) by mechanical disruption using 100 μ m strainers (Corning, NY, USA). To stain for CD79a and CD79b protein, 2×10^6 cells were incubated in MACS buffer (PBS/0.5% BSA/2mM EDTA) with combinations of monoclonal antibodies (Supporting information Table S1) and stained according to previously described procedures [42] and adhered to general guidelines for flow cytometry [61]. To detect CD79a protein intracellularly, cells were fixed using 2% paraformaldehyde (PFA) in PBS and permeabilized using 0.5% Saponin (Sigma Aldrich, St. Louis, MO, USA) in MACS buffer.

To measure activation of antiapoptotic and survival pathways, 0.5×10^6 splenic cells were cultured in RPMI-5% FCS at 37°C for 22 h for Bcl-XL (Cell Signaling Technologies, Danvers, MA, USA), Mcl-1 (Abcam, Cambridge, UK), and c-Rel (Miltenyi Biotec, Bergisch Gladbach, Germany), or 1 h for I κ B α (Invitrogen, Waltham, MA, USA) expression. Splenic cells were stimulated with 25 μ g/mL anti-mouse antigen-binding F(ab')₂-IgM fragments (anti-IgM; Jackson ImmunoResearch, West Grove, PA, USA) or left unstimulated. Subsequently, cells were stained for cell surface markers and viability on ice in the dark. To detect intracellular proteins, we fixed the cells with 2% PFA in PBS for 10

min followed by permeabilization using 0.5% Saponin in MACS buffer.

To measure intracellular calcium mobilization, 5×10^6 splenocytes were incubated with Fluo3-AM and Fura Red-AM fluorogenic probes (Life Technologies, Carlsbad, CA, USA), as previously described [34, 36]. During measurements, cells were stimulated with 25 μ g/mL anti-IgM after running a 30 s baseline.

Upon completion of the staining procedure, samples were measured in MACS buffer on an LSR-II (BD Biosciences, San Jose, CA, USA) and analyzed using FlowJo v10 (BD Biosciences).

Phosphoflow cytometry

For phosphoflow experiments, 0.5×10^6 cells were cultured in RPMI-2% FCS at 37°C for 1 min for pPI3K p85 (Cell Signaling Technologies), 3 min for pSHP-1 (Cell Signaling Technologies), 5 min for pSrc (Abcam), pLyn (Abwiz Bio, San Diego, CA, USA), pCD79a (Cell Signaling Technologies), pSyk, pSLP-65, pPLC γ 2, and pErk (all BD Biosciences) or for 3 h for pS6 and pAkt (both Cell Signaling Technologies) with 25 μ g/mL anti-IgM or antigen-binding F(ab')₂-Ig κ fragments (anti-IgK; Jackson ImmunoResearch). After fixation with the eBioscience FoxP3 staining kit Fix/Perm solution, cells were washed twice with the accompanying Perm/Wash solution (Invitrogen). Next, cells were incubated with varying combinations of monoclonal antibodies (Supporting information Table S1) and stained according to previously described procedures [31]. After staining for the phosphoproteins, samples were measured in MACS buffer on an LSR-II (BD Biosciences) and analyzed using FlowJo v10 (BD Biosciences).

In vitro and in vivo treatment with acalabrutinib

In vitro cultures were performed by pretreating 0.5×10^6 splenic cells with 1 μ M acalabrutinib (ACP-196; MedChemExpress, Monmouth Junction, NJ, USA) or 1 μ M DMSO in RPMI-2% FCS for 3 h at 37°C. Cells were subsequently stimulated with 25 μ g/mL anti-IgM or alternatively RPMI-2% FCS was added as unstimulated control.

For single-dose experiments for in vivo Btk-kinase inhibition, CBA/J WT mice were treated with one dose of 25 mg/kg acalabrutinib in vehicle solution (Trappsol@Cyclo (2-Hydroxypropyl-beta-cyclodextrin [HP β CD])); CTD inc, Gainesville, FL, USA) or vehicle alone by oral gavage. Mice were sacrificed 3 h after acalabrutinib administration.

For prolonged in vivo treatment, CBA/J WT mice received 0.16 mg/mL acalabrutinib diluted in vehicle or vehicle alone formulated in drinking water [39] for 5 days, which corresponds with administration of a daily dose of 25 mg/kg.

Adoptive transfer EMC6 in *Rag1*^{-/-} mice and ibrutinib treatment

To study the effects of Btk inhibitors on BCR signaling in leukemia, 1×10^6 cells EMC6 CLL cells—a cell line derived from the *IgH.TE μ* CLL mouse model [35]—were intraperitoneally injected into *Rag1*^{-/-} mice [36]. Mice were monitored for the onset of leukemia by blood screening and randomized into different groups based on the percentage of leukemic cells in circulation prior to treatment, as previously described [38]. After 12 days, EMC6-engrafted *Rag1*^{-/-} mice received 0.16 mg/mL ibrutinib [62] diluted in vehicle or vehicle alone formulated in drinking water for 14 days. After 14 days of treatment, mice again received regular drinking water. Mice were euthanized upon development of severe signs of disease, for example, difficulty to breath and aversion to activity, or at the experimental end-point of 20 days after start of ibrutinib treatment.

Statistical analysis

Statistical differences were calculated in GraphPad Prism 5 software (GraphPad Software Inc; San Diego, CA, USA) by Mann–Whitney *U* test or Kruskal–Wallis test with Dunn's multiple comparison posthoc test. A Log Rank test was performed to calculate difference in survival for CLL-engrafted *Rag1*^{-/-} mice. *p* values <0.05 were considered significant.

Acknowledgments: We would like to thank Jelle Bolier, Tobias Defesche (Erasmus MC Rotterdam), and the EDC Erasmus MC animal facility for their great technical assistance. These studies were partially supported by the Dutch Arthritis Foundation (Grant number 19-1-201), Dutch Cancer Society (KWF Grant 2014–6564), and Target-to-B, all awarded to R.W. Hendriks.

Author contributions: JR designed the research, performed experiments, analyzed the data, and wrote the manuscript. MdB, SN, SPS, JW, and JvH performed experiments and analyzed the data. OC and RH contributed to the research design and the writing of the manuscript and supervised the study. All coauthors approved the final manuscript.

Conflict of interests: The authors declare to have no financial or commercial conflicts of interest.

Peer review: The peer review history for this article is available at <https://publons.com/publon/10.1002/eji.202048968>

Data availability statement: The data that supports these findings are available from the corresponding author upon reasonable request.

References

- Kraus, M., Alimzhanov, M. B., Rajewsky, N. and Rajewsky, K., Survival of resting mature B lymphocytes depends on BCR signaling via the Igalpha/beta heterodimer. *Cell* 2004. 117: 787–800.
- Rip, J., Van Der Ploeg, E. K., Hendriks, R. W. and Corneth, O. B. J., The role of Bruton's tyrosine kinase in immune cell signaling and systemic autoimmunity. *Crit. Rev. Immunol.* 2018. 38: 17–62.
- Pal Singh, S., Dammeijer, F. and Hendriks, R. W., Role of Bruton's tyrosine kinase in B cells and malignancies. *Mol. Cancer* 2018. 17: 57.
- Wang, M. L., Rule, S., Martin, P., Goy, A., Auer, R., Kahl, B. S., Jurczak, W. et al., Targeting BTK with ibrutinib in relapsed or refractory mantle-cell lymphoma. *N. Engl. J. Med.* 2013. 369: 507–516.
- Byrd, J. C., Furman, R. R., Coutre, S. E., Flinn, I. W., Burger, J. A., Blum, K. A., Grant, B., et al., Targeting BTK with ibrutinib in relapsed chronic lymphocytic leukemia. *N. Engl. J. Med.* 2013. 369: 32–42.
- Byrd, J. C., Harrington, B., O'Brien, S., Jones, J. A., Schuh, A., Devereux, S., Chaves, J. et al., Acalabrutinib (ACP-196) in relapsed chronic lymphocytic leukemia. *N. Engl. J. Med.* 2016. 374: 323–332.
- Montalban, X., Arnold, D. L., Weber, M. S., Staikov, I., Piasecka-Stryczynska, K., Willmer, J., Martin, E. C. et al., Placebo-controlled trial of an oral BTK inhibitor in multiple sclerosis. *New England Journal of Medicine* 2019. 380: 2406–2417.
- Vetrie, D., Vorechovsky, I., Sideras, P., Holland, J., Davies, A., Flinter, F., Hammarstrom, L. et al., The gene involved in X-linked agammaglobulinemia is a member of the src family of protein-tyrosine kinases. *Nature* 1993. 361: 226–233.
- Tsukada, S., Saffran, D. C., Rawlings, D. J., Parolini, O., Allen, R. C., Klisak, I., Sparkes, R. S. et al., Deficient expression of a B cell cytoplasmic tyrosine kinase in human X-linked agammaglobulinemia. *Cell* 1993. 72: 279–290.
- Khan, W. N., Alt, F. W., Gerstein, R. M., Malynn, B. A., Larsson, I., Rathbun, G., Davidson, L. et al., Defective B cell development and function in Btk-deficient mice. *Immunity* 1995. 3: 283–299.
- Middendorp, S., Dingjan, G. M. and Hendriks, R. W., Impaired precursor B cell differentiation in Bruton's tyrosine kinase-deficient mice. *J. Immunol.* 2002. 168: 2695–2703.
- Rawlings, D. J., Saffran, D. C., Tsukada, S., Largaespada, D. A., Grimaldi, J. C., Cohen, L., Mohr, R. N. et al., Mutation of unique region of Bruton's tyrosine kinase in immunodeficient XID mice. *Science* 1993. 261: 358–361.
- Jumaa, H., Mitterer, M., Reth, M. and Nielsen, P. J., The absence of SLP65 and Btk blocks B cell development at the preB cell receptor-positive stage. *Eur. J. Immunol.* 2001. 31: 2164–2169.
- Ellmeier, W., Jung, S., Sunshine, M. J., Hatam, F., Xu, Y., Baltimore, D., Mano, H. et al., Severe B cell deficiency in mice lacking the TEC kinase family members TEC and Btk. *J. Exp. Med.* 2000. 192: 1611–1624.
- Nyhoff, L. E., Clark, E. S., Barron, B. L., Bonami, R. H., Khan, W. N. and Kendall, P. L., Bruton's tyrosine kinase is not essential for B cell survival beyond early developmental stages. *J. Immunol.* 2018. 200: 2352–2361.
- Burger, J. A., Barr, P. M., Robak, T., Owen, C., Ghia, P., Tedeschi, A., Bairey, O. et al., Long-term efficacy and safety of first-line ibrutinib treatment for patients with CLL/SLL: 5 years of follow-up from the phase 3 RESONATE-2 study. *Leukemia* 2020. 34: 787–798.
- George, B., Chowdhury, S. M., Hart, A., Sircar, A., Singh, S. K., Nath, U. K., Mamgain, M. et al., Ibrutinib resistance mechanisms and treatment strategies for B-cell lymphomas. *Cancers (Basel)* 2020. 12: 1328.
- Rebecca, V. W. and Smalley, K. S., Change or die: targeting adaptive signaling to kinase inhibition in cancer cells. *Biochem. Pharmacol.* 2014. 91: 417–425.

- 19 Pratilas, C. A., Taylor, B. S., Ye, Q., Viale, A., Sander, C., Solit, D. B. and Rosen, N., (V600E)BRAF is associated with disabled feedback inhibition of RAF-MEK signaling and elevated transcriptional output of the pathway. *Proc. Natl. Acad. Sci. U. S. A.* 2009. **106**: 4519–4524.
- 20 Kil, L. P., de Bruijn, M. J., van Hulst, J. A., Langerak, A. W., Yuvaraj, S. and Hendriks, R. W., Bruton's tyrosine kinase mediated signaling enhances leukemogenesis in a mouse model for chronic lymphocytic leukemia. *Am J Blood Res* 2013. **3**: 71–83.
- 21 Corneth, O. B. J., Verstappen, G. M. P., Paulissen, S. M. J., de Bruijn, M. J. W., Rip, J., Lukkes, M., van Hamburg, J. P. et al., Enhanced Bruton's tyrosine kinase activity in peripheral blood B lymphocytes from patients with autoimmune disease. *Arthritis Rheumatol* 2017. **69**: 1313–1324.
- 22 Schmid, C., Vladimer, G. I., Rendeiro, A. F., Schnabl, S., Krausgruber, T., Taubert, C., Krall, N. et al., Combined chemosensitivity and chromatin profiling prioritizes drug combinations in CLL. *Nat. Chem. Biol.* 2019. **15**: 232–240.
- 23 Bajpai, U. D., Zhang, K., Teutsch, M., Sen, R. and Wortis, H. H., Bruton's tyrosine kinase links the B cell receptor to nuclear factor kappaB activation. *J. Exp. Med.* 2000. **191**: 1735–1744.
- 24 Petro, J. B., Rahman, S. M., Ballard, D. W. and Khan, W. N., Bruton's tyrosine kinase is required for activation of IkappaB kinase and nuclear factor kappaB in response to B cell receptor engagement. *J. Exp. Med.* 2000. **191**: 1745–1754.
- 25 Petlickovski, A., Laurenti, L., Li, X., Marietti, S., Chiusolo, P., Sica, S., Leone, G. et al., Sustained signaling through the B-cell receptor induces Mcl-1 and promotes survival of chronic lymphocytic leukemia B cells. *Blood* 2005. **105**: 4820–4827.
- 26 Saijo, K., Mecklenbrauker, I., Santana, A., Leitger, M., Schmedt, C. and Tarakhovskiy, A., Protein kinase C beta controls nuclear factor kappaB activation in B cells through selective regulation of the IkappaB kinase alpha. *J. Exp. Med.* 2002. **195**: 1647–1652.
- 27 Ingley, E., Src family kinases: regulation of their activities, levels and identification of new pathways. *Biochim. Biophys. Acta* 2008. **1784**: 56–65.
- 28 Perez-Villar, J. J., Whitney, G. S., Bowen, M. A., Hewgill, D. H., Aruffo, A. A. and Kanner, S. B., CD5 negatively regulates the T-cell antigen receptor signal transduction pathway: involvement of SH2-containing phosphotyrosine phosphatase SHP-1. *Mol. Cell. Biol.* 1999. **19**: 2903–2912.
- 29 Otipoby, K. L., Draves, K. E. and Clark, E. A., CD22 regulates B cell receptor-mediated signals via two domains that independently recruit Grb2 and SHP-1. *J. Biol. Chem.* 2001. **276**: 44315–44322.
- 30 Hoffmann, A., Kerr, S., Jellusova, J., Zhang, J., Weisel, F., Wellmann, U., Winkler, T. H. et al., Siglec-G is a B1 cell-inhibitory receptor that controls expansion and calcium signaling of the B1 cell population. *Nat. Immunol.* 2007. **8**: 695–704.
- 31 Rip, J., de Bruijn, M. J. W., Kaptein, A., Hendriks, R. W. and Corneth, O. B. J., Phosphoflow protocol for signaling studies in human and murine B cell subpopulations. *J. Immunol.* 2020. **204**: 2852–2863.
- 32 Scher, I., The CBA/N mouse strain: an experimental model illustrating the influence of the X-chromosome on immunity. *Adv. Immunol.* 1982. **33**: 1–71.
- 33 Hendriks, R. W., de Bruijn, M. F., Maas, A., Dingjan, G. M., Karis, A. and Grosveld, F., Inactivation of Btk by insertion of lacZ reveals defects in B cell development only past the pre-B cell stage. *EMBO J.* 1996. **15**: 4862–4872.
- 34 Rip, J., de Bruijn, M. J. W., Appelman, M. K., Pal Singh, S., Hendriks, R. W. and Corneth, O. B. J., Toll-like receptor signaling drives Btk-mediated autoimmune disease. *Front. Immunol.* 2019. **10**: 95.
- 35 ter Brugge, P. J., Ta, V. B., de Bruijn, M. J., Keijzers, G., Maas, A., van Gent, D. C. and Hendriks, R. W., A mouse model for chronic lymphocytic leukemia based on expression of the SV40 large T antigen. *Blood* 2009. **114**: 119–127.
- 36 Singh, S. P., Pillai, S. Y., de Bruijn, M. J. W., Stadhouders, R., Corneth, O. B. J., van den Ham, H. J., Muggen, A. et al., Cell lines generated from a chronic lymphocytic leukemia mouse model exhibit constitutive Btk and Akt signaling. *Oncotarget* 2017. **8**: 71981–71995.
- 37 Craxton, A., Jiang, A., Kurosaki, T. and Clark, E. A., Syk and Bruton's tyrosine kinase are required for B cell antigen receptor-mediated activation of the kinase Akt. *J. Biol. Chem.* 1999. **274**: 30644–30650.
- 38 de Rooij, M. F., Kuil, A., Geest, C. R., Eldering, E., Chang, B. Y., Buggy, J. J., Pals, S. T. et al., The clinically active BTK inhibitor PCI-32765 targets B-cell receptor- and chemokine-controlled adhesion and migration in chronic lymphocytic leukemia. *Blood* 2012. **119**: 2590–2594.
- 39 Herman, S. E. M., Montraveta, A., Niemann, C. U., Mora-Jensen, H., Gulrajani, M., Krantz, F., Mantel, R. et al., The Bruton tyrosine kinase (BTK) inhibitor acalabrutinib demonstrates potent on-target effects and efficacy in two mouse models of chronic lymphocytic leukemia. *Clin. Cancer Res.* 2017. **23**: 2831–2841.
- 40 Rigley, K. P., Harnett, M. M., Phillips, R. J. and Klaus, G. G., Analysis of signaling via surface immunoglobulin receptors on B cells from CBA/N mice. *Eur. J. Immunol.* 1989. **19**: 2081–2086.
- 41 Fluckiger, A. C., Li, Z., Kato, R. M., Wahl, M. I., Ochs, H. D., Longnecker, R., Kinet, J. P. et al., Btk/Tec kinases regulate sustained increases in intracellular Ca²⁺ following B-cell receptor activation. *EMBO J.* 1998. **17**: 1973–1985.
- 42 Kil, L. P., de Bruijn, M. J., van Nimwegen, M., Corneth, O. B., van Hamburg, J. P., Dingjan, G. M., Thaiss, F. et al., Btk levels set the threshold for B-cell activation and negative selection of autoreactive B cells in mice. *Blood* 2012. **119**: 3744–3756.
- 43 Berry, C. T., Liu, X., Myles, A., Nandi, S., Chen, Y. H., Hershberg, U., Brodsky, I. E. et al., BCR-induced Ca(2+) signals dynamically tune survival, metabolic reprogramming, and proliferation of naive B Cells. *Cell Rep.* 2020. **31**: 107474.
- 44 Rowland, S. L., DePersis, C. L., Torres, R. M. and Pelanda, R., Ras activation of Erk restores impaired tonic BCR signaling and rescues immature B cell differentiation. *J. Exp. Med.* 2010. **207**: 607–621.
- 45 Moyo, T. K., Wilson, C. S., Moore, D. J. and Eischen, C. M., Myc enhances B-cell receptor signaling in precancerous B cells and confers resistance to Btk inhibition. *Oncogene* 2017. **36**: 4653–4661.
- 46 Whillock, A. L., Ybarra, T. K. and Bishop, G. A., TNF receptor-associated factor 3 restrains B cell receptor signaling in normal and malignant B cells. *J. Biol. Chem.* 2021: 100465.
- 47 Linley, A., Karydis, L., Mondru, A., D'Avola, A., Cicconi, S., Griffin, R., Forconi, F. et al., Kinobead profiling reveals reprogramming of B-cell receptor signaling in response to therapy within primary chronic lymphocytic leukemia cells. *bioRxiv* 2020: 841312. <https://doi.org/10.1101/841312>
- 48 Noviski, M., Mueller, J. L., Satterthwaite, A., Garrett-Sinha, L. A., Brombacher, F. and Zikherman, J., IgM and IgD B cell receptors differentially respond to endogenous antigens and control B cell fate. *Elife* 2018. **7**.
- 49 Sabouri, Z., Perotti, S., Spierings, E., Humburg, P., Yabas, M., Bergmann, H., Horikawa, K. et al., IgD attenuates the IgM-induced anergy response in transitional and mature B cells. *Nat. Commun.* 2016. **7**: 13381.
- 50 Brouns, G. S., de Vries, E. and Borst, J., Assembly and intracellular transport of the human B cell antigen receptor complex. *Int. Immunol.* 1995. **7**: 359–368.
- 51 He, X., Klasener, K., Iype, J. M., Becker, M., Maity, P. C., Cavallari, M., Nielsen, P. J. et al., Continuous signaling of CD79b and CD19 is

- required for the fitness of Burkitt lymphoma B cells. *EMBO J.* 2018. 37.
- 52 Hendriks, R. W., Yuvaraj, S. and Kil, L. P., Targeting Bruton's tyrosine kinase in B cell malignancies. *Nat. Rev. Cancer* 2014. 14: 219–232.
- 53 Stadhouders, R., de Bruijn, M. J., Rother, M. B., Yuvaraj, S., Ribeiro de Almeida, C., Kolovos, P., Van Zelm, M. C. et al., Pre-B cell receptor signaling induces immunoglobulin kappa locus accessibility by functional redistribution of enhancer-mediated chromatin interactions. *PLoS Biol.* 2014. 12: e1001791.
- 54 Deng, J., Isik, E., Fernandes, S. M., Brown, J. R., Letai, A. and Davids, M. S., Bruton's tyrosine kinase inhibition increases BCL-2 dependence and enhances sensitivity to venetoclax in chronic lymphocytic leukemia. *Leukemia* 2017. 31: 2075–2084.
- 55 Eyre, T. A., Walter, H. S., Iyengar, S., Follows, G., Cross, M., Fox, C. P., Hodson, A., Coats, J. et al., Efficacy of venetoclax monotherapy in patients with relapsed, refractory mantle cell lymphoma after Bruton tyrosine kinase inhibitor therapy. *Haematologica* 2019. 104: e68–e71.
- 56 Honigberg, L. A., Smith, A. M., Sirisawad, M., Verner, E., Loury, D., Chang, B., Li, S. et al., The Bruton tyrosine kinase inhibitor PCI-32765 blocks B-cell activation and is efficacious in models of autoimmune disease and B-cell malignancy. *Proc. Natl. Acad. Sci. U. S. A.* 2010. 107: 13075–13080.
- 57 Haselmayer, P., Camps, M., Liu-Bujalski, L., Nguyen, N., Morandi, F., Head, J., O'Mahony, A. et al., Efficacy and pharmacodynamic modeling of the BTK inhibitor evobrutinib in autoimmune disease models. *J. Immunol.* 2019. 202: 2888–2906.
- 58 Roschewski, M., Lionakis, M. S., Sharman, J. P., Roswarski, J., Goy, A., Monticelli, M. A., Roshon, M. et al., Inhibition of Bruton tyrosine kinase in patients with severe COVID-19. *Science Immunology* 2020. 5: eabd0110.
- 59 Maas, A., Dingjan, G. M., Grosveld, F. and Hendriks, R. W., Early arrest in B cell development in transgenic mice that express the E41K Bruton's tyrosine kinase mutant under the control of the CD19 promoter region. *J. Immunol.* 1999. 162: 6526–6533.
- 60 Mombaerts, P., Iacomini, J., Johnson, R. S., Herrup, K., Tonegawa, S. and Papaioannou, V. E., RAG-1-deficient mice have no mature B and T lymphocytes. *Cell* 1992. 68: 869–877.
- 61 Cossarizza, A., Chang, H. D., Radbruch, A., Acs, A., Adam, D., Adam-Klages, S., Agace, W. W. et al., Guidelines for the use of flow cytometry and cell sorting in immunological studies (second edition). *Eur. J. Immunol.* 2019. 49: 1457–1973.
- 62 Woyach, J. A., Bojnik, E., Ruppert, A. S., Stefanovski, M. R., Goettl, V. M., Smucker, K. A., Smith, L. L. et al., Bruton's tyrosine kinase (BTK) function is important to the development and expansion of chronic lymphocytic leukemia (CLL). *Blood* 2014. 123: 1207–1213.

Abbreviations: **Btk/BTK:** Bruton's tyrosine kinase · **CLL:** Chronic Lymphocytic Leukemia · **gMFI:** geometric mean fluorescence intensity · **MCL:** Mantle-cell lymphoma · **MZ:** Marginal zone · **T1:** Transitional type 1

Full correspondence: Prof. Rudi W. Hendriks, Department of Pulmonary Medicine, Room Ee2251a, Erasmus MC Rotterdam, PO Box 2040, NL 3000 CA Rotterdam, The Netherlands.
Email: r.hendriks@erasmusmc.nl
Dr. Odilia B. J. Corneth
Email: o.corneth@erasmusmc.nl

Current address: Jasper Rip, Department of Immunology, Erasmus MC, University Medical Center Rotterdam.

Received: 11/9/2020
Revised: 31/3/2021
Accepted: 22/7/2021
Accepted article online: 29/7/2021